This article has been accepted for inclusion in a future issue of this journal. Content is final as presented, with the exception of pagination.

Power System State Estimation Using PMUs With Imperfect Synchronization

Peng Yang, *Student Member, IEEE*, Zhao Tan, *Student Member, IEEE*, Ami Wiesel, *Member, IEEE*, and Arye Nehorai, *Fellow, IEEE*

***Abstract*—Phasor measurement units (PMUs) are time synchronized sensors primarily used for power system state estimation. Despite their increasing incorporation and the ongoing research on state estimation using measurements from these sensors, estimation with imperfect phase synchronization has not been sufficiently investigated. Inaccurate synchronization is an inevitable problem that large scale deployment of PMUs has to face. In this paper, we introduce a model for power system state estimation using PMUs with phase mismatch. We propose alternating minimization and parallel Kalman filtering for state estimation using static and dynamic models, respectively, under different assumptions. Numerical examples demonstrate the improved accuracy of our algorithms compared with traditional algorithms when imperfect synchronization is present. We conclude that when a sufficient number of PMUs with small delays are employed, the imperfect synchronization can be largely compensated in the estimation stage.**

***Index Terms*—Alternating minimization (AM), bilinear model, Kalman filtering, phase mismatch, phasor measurement unit (PMU), state estimation, synchronization.**

NOMENCLATURE:

PMU	Phasor measurement unit.
SCADA	Supervisory control and data acquisition.
GPS	Global positioning system.
PTP	Precision time protocol.
WWVB	Time signal radio station located in Colorado, USA.
DSE	Dynamic state estimation.
SSE	Static state estimation.
MAP	Maximum *a posteriori*.
OKF	Kalman filtering with perfect information of time delay (the oracle case).
OLF	Least squares estimation with perfect information of time delay (the oracle case).
PKF	Parallel Kalman filtering.
STLS	Structured total least squares.
SVD	Singular value decomposition.
TLS	Total least squares.
WLS	Weighted least squares.

Manuscript received October 10, 2012; revised February 20, 2013; accepted June 27, 2013. The work of A. Wiesel was supported by the Israel Smart Grid (ISG) consortium. The work of A. Nehorai was supported in part by the Department of Defense under the AFOSR Grant FA9550-11-1-0210. Paper no. TPWRS-01147-2012.

P. Yang, Z. Tan, and A. Nehorai are with the Preston M. Green Department of Electrical and Systems Engineering, Washington University in St. Louis, St. Louis, MO 63130 USA (e-mail: yangp@ese.wustl.edu; tanz@ese.wustl.edu; nehorai@ese.wustl.edu).

A. Wiesel is with the Hebrew University of Jerusalem, Jerusalem 91904, Israel. (e-mail: amiw@cs.huji.ac.il).

Color versions of one or more of the figures in this paper are available online at http://ieeexplore.ieee.org.

Digital Object Identifier 10.1109/TPWRS.2013.2272220

I. INTRODUCTION

In recent years, phasor measurement units (PMUs) [1] have become increasingly important in power system state estimation [2]–[7]. The traditional supervisory control and data acquisition (SCADA) system has a low reporting rate and requires complex nonlinear state estimation, since the SCADA measurements, e.g., the power flow and power injections, are nonlinear functions of the system states (complex bus voltages). PMUs provide synchronized phasor measurement, which results in linear models for state estimation. Their sampling rate is much higher, enabling real-time estimation of the power system's state and fast response to abnormalities. There has been ongoing research on state estimation using PMUs [8]–[13]. Most of the recent work directly combines the SCADA data with data from PMUs and uses weighted least-squares (WLS) estimation and similar methods. One important issue with this approach is that the SCADA measurements are not synchronized, and the sample rates of SCADA and PMUs are different, causing the time skewness problem [14].

Typically, PMUs use a global positioning system (GPS) radio clock, which sends a one pulse per second (1 pps) synchronization signal [15]. Currently, the deployment of PMUs is limited due to various reasons. Optimal placement of PMUs has recently been investigated to permit installation of a minimum number of PMUs [16]–[18]. However, without enough PMUs, their advantage in linear measurements and high reporting rate cannot be fully exploited, and traditional low-sample-rate nonlinear measurements still have to be used for full system state estimation.

Large-scale deployment of PMUs inevitably result in the use of PMUs from multiple vendors. However, due to different standards, protocols, and designs, the synchronization of PMUs from different vendors is a problem. According to [19], the clocks of PMUs need to be accurate to 500 ns to provide the 1-ms time standard needed by each device performing synchrophasor measurement. The accurate and consistency of all PMUs, regardless of their makes and models, is important for large-scale PMU deployments [20]. However, a test shows that

PMUs from multiple vendors can yield errors of about 47 ms in time synchronization [21]. In addition, in large-scale deployments, PMUs with alternative but less accurate synchronization mechanism may be used. These alternative synchronization mechanisms may include the Precision Time Protocol (PTP) as defined in IEEE-1588 standard [22]–[24], or time signal radio stations, e.g., WWVB located in Colorado, U.S. [25]. According to the IEEE-1588 standard, instead of purely using a GPS radio clock for each of the devices, only the "masters" are equipped with global clocks. The "slaves" use local clocks, and a sync message is transmitted from a "master" to its "slaves" every few seconds. Alternatively, the WWVB radio station uses a pulse amplitude modulated signal with a bit rate of 1 b/s to synchronize widely separated clocks, with lower accuracy compared with GPS radio clocks. As a general model, in this paper, we consider different PMUs are synchronized every $T_{\rm sync}$ seconds and use imperfect local clocks between consecutive synchronizations.

When the PMUs are not perfectly synchronized, the traditional measurement model which considers the phase mismatch resulting from dissynchronization as additive noise is no longer accurate. In fact, as our numerical example suggests, if the synchronization error and/or the time between consecutive synchronizations increase, the traditional estimation methods will deteriorate significantly. To mitigate this problem, we introduce a new model for state estimation with consideration of PMU phase mismatch. We propose estimation algorithms based on alternating minimization (AM) and parallel Kalman filtering (PKF) [26] for estimation using the static and dynamic models, respectively. The estimation algorithm based on the static model is simple and robust and does not require any assumptions on the dynamics of the states and phase mismatch. The filtering approach is preferable for tracking time-varying phase mismatches under the standard dynamic state space model, as it is less computationally intensive. Numerical examples demonstrate that our proposed algorithms provide more accurate state estimates when the PMUs are imperfectly synchronized. The estimation performance remain satisfactory when the synchronization error increases. We conclude that, when a sufficient number of PMUs are employed and the mismatches are small, our methods can largely compensate for the errors resulting from imperfect time synchronization.

The remainder of this paper is organized as follows. In Section II, we describe the measurement and system model considering phase mismatch. In Section III, we introduce the proposed algorithms for state estimation with phase mismatch. We show numerical examples in Section IV and conclude the paper in Section V.

Notations: we use superscript c to denote continuous signals, $\{\cdot\}^{\rm r}$ to denote the real part, $\{\cdot\}^{\rm i}$ to denote the imaginary part, superscript T to denote vector transpose, $\mathrm{card}(\cdot)$ to denote the cardinality of a set, and $\mathrm{mod}(\cdot,\cdot)$ to denote the modulo operator.

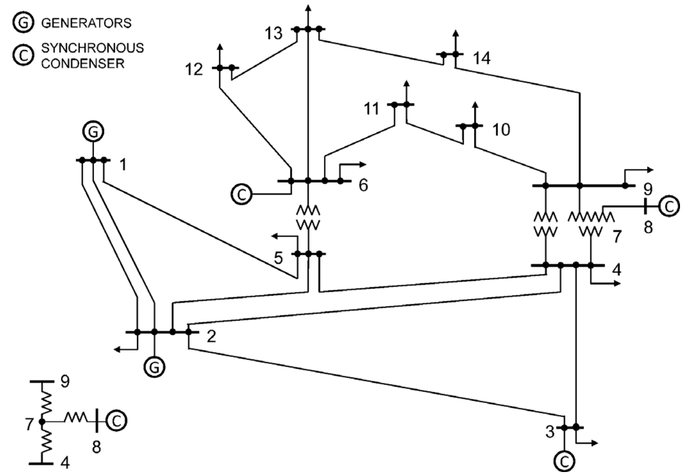

Fig. 1. IEEE 14-bus system.

II. Measurement and System Model

A. Measurement Model

We consider a grid model with N buses connected via branches, e.g., the IEEE 14-bus model in Fig. 1. The continuous voltage signal on bus p at time instance $t \in \mathbb{R}^+$ is defined as

$$\overline{E}_p^c(t) = E_p^c(t)\cos\left(2\pi f_c t + \varphi_p^c(t)\right) \tag{1}$$

where f_c is the frequency. The phasor representation of $\overline{E}_p^c(t)$ is $E_p^c(t)e^{j\varphi_p^c(t)}$, where $E_p^c(t)$ denotes the magnitude and $\varphi_p^c(t)$ denotes the phase. For simplicity, we work with discrete phasor time series

$$\begin{aligned} E_{p,k} &= E_p^c(kT) \\ \varphi_{p,k} &= \varphi_p^c(kT) \end{aligned} \tag{2}$$

where T is the PMU reporting period, which is typically around tens of milliseconds, and $k \in \mathbb{N}^+$. In Cartesian coordinates, this translates to

$$E_{p,k}^{\rm r} = E_{p,k}\cos\varphi_{p,k} \tag{3}$$

$$E_{p,k}^{\rm i} = E_{p,k}\sin\varphi_{p,k}. \tag{4}$$

We define the state of the power grid at time instance k as a length-$2N$ real valued vector

$$\boldsymbol{s}_k = [E_{1,k}^{\rm r}, E_{1,k}^{\rm i}, E_{2,k}^{\rm r}, E_{2,k}^{\rm i}, \ldots, E_{N,k}^{\rm r}, E_{N,k}^{\rm i}]^T. \tag{5}$$

The voltages on the buses are related to the currents through the branches, as illustrated in Fig. 2. We denote the susceptance at bus p as B_p and the admittance at branch $\{p,q\}$ as y_{pq}, with

$$y_{pq} = g_{pq} + j \cdot b_{pq} \tag{6}$$

where g_{pq} is the conductance and b_{pq} is the susceptance. These parameters are assumed to be known and constant.

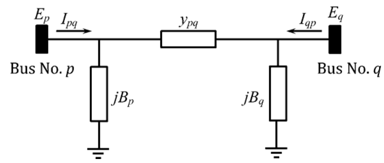

Fig. 2. Bus branch model.

Consequently, the real and imaginary parts of the current on branch $\{p,q\}$ are given by

$$I^{\mathrm{r}}_{pq,k} = \left(E^{\mathrm{r}}_{p,k} - E^{\mathrm{r}}_{q,k}\right) g_{pq} - \left(E^{\mathrm{i}}_{p,k} - E^{\mathrm{i}}_{q,k}\right) b_{pq} - B_p E^{\mathrm{i}}_{p,k} \quad (7)$$

$$I^{\mathrm{i}}_{pq,k} = \left(E^{\mathrm{r}}_{p,k} - E^{\mathrm{r}}_{q,k}\right) b_{pq} + \left(E^{\mathrm{i}}_{p,k} - E^{\mathrm{i}}_{q,k}\right) g_{pq} + B_p E^{\mathrm{r}}_{p,k}. \quad (8)$$

To avoid the time skewness problems with traditional SCADA estimation, in this paper, we consider state estimation using only PMUs. An alternative approach is to incorporate SCADA estimation as priors for the estimation based on PMU data [16], which could be easily incorporated into our model. In an ideal setting, the power system is monitored via a network of M perfectly synchronized PMUs measuring the voltages and currents located in a set of buses $\mathcal{M}$ at time stamps kT for $k \in \mathbb{N}^+$, where $M = \mathrm{card}(\mathcal{M})$. The PMU installed on the pth bus measures noisy versions of

$$\tilde{\boldsymbol{z}}^p_k = \boldsymbol{H}_p \boldsymbol{s}^p_k \quad (9)$$

with

$$\tilde{\boldsymbol{z}}^p_k = \left[E^{\mathrm{r}}_{p,k}, E^{\mathrm{i}}_{p,k}, I^{\mathrm{r}}_{pq_1,k}, I^{\mathrm{i}}_{pq_1,k}, \ldots, I^{\mathrm{r}}_{pq_u,k}, I^{\mathrm{i}}_{pq_u,k}\right]^T$$

$$\boldsymbol{s}^p_k = \left[E^{\mathrm{r}}_{p,k}, E^{\mathrm{i}}_{p,k}, E^{\mathrm{r}}_{q_1,k}, E^{\mathrm{i}}_{q_1,k}, \ldots, E^{\mathrm{r}}_{q_u,k}, E^{\mathrm{i}}_{q_u,k}\right]^T$$

where $q_1, \ldots, q_u$ are the indices of the neighboring buses to bus p. The matrix $\boldsymbol{H}_p$ can be written as

$$\boldsymbol{H}_p = \begin{bmatrix} \mathbf{I} & \mathbf{0} & \cdots & \mathbf{0} \\ \boldsymbol{\Upsilon}_{pq_1} & \tilde{\boldsymbol{\Upsilon}}_{pq_1} & \cdots & \mathbf{0} \\ \vdots & \vdots & \ddots & \vdots \\ \boldsymbol{\Upsilon}_{pq_u} & \mathbf{0} & \cdots & \tilde{\boldsymbol{\Upsilon}}_{pq_u} \end{bmatrix} \quad (10)$$

where

$$\boldsymbol{\Upsilon}_{pq_i} = \begin{bmatrix} g_{pq_i} & -b_{pq_i} - B_p \\ b_{pq_i} + B_p & -b_{pq_i} \end{bmatrix} \quad (11)$$

$$\tilde{\boldsymbol{\Upsilon}}_{pq_i} = \begin{bmatrix} -g_{pq_i} & b_{pq_i} \\ -b_{pq_i} & -g_{pq_i} \end{bmatrix}. \quad (12)$$

Stacking the noisy versions of (9) for all $p \in \mathcal{M}$ into one large model yields the traditional power grid observation model

$$\boldsymbol{z}_k = \tilde{\boldsymbol{z}}_k + \boldsymbol{\epsilon}_k = \boldsymbol{H}\boldsymbol{s}_k + \boldsymbol{\epsilon}_k \quad (13)$$

where $\tilde{\boldsymbol{z}}^p_k$, $\boldsymbol{H}_p$, and $\boldsymbol{s}^p_k$ are the appropriate subblocks of $\tilde{\boldsymbol{z}}_k$, $\boldsymbol{H}$, and $\boldsymbol{s}_k$ corresponding to the PMU on the pth bus, and $\boldsymbol{\epsilon}_k$ denotes Gaussian measurement noise with $\boldsymbol{\epsilon}_k \sim \mathcal{N}(\mathbf{0}, \boldsymbol{R}_{\epsilon,k})$. In a common case where the noise is independent identically distributed (i.i.d.), $\boldsymbol{R}_{\epsilon,k} = \sigma^2\mathbf{I}$.

We now propose a more realistic state space model which takes into account the imperfect synchronization of the PMUs. The PMU installed on the pth bus measures its kth sample at time $kT + t_{p,k}$, where $t_{p,k}$ is the time delay of the pth PMU at the kth sample. Denote the delays of all PMUs as a vector $\boldsymbol{t}_k = [\ldots, t_{p,k}, \ldots]^T$, where $p \in \mathcal{M}$.

The voltage at bus p at time instance $kT + t_{p,k}$ is

$$\begin{aligned} \overline{E}^c_p(kT + t_{p,k}) &= E^c_p(kT + t_{p,k}) \\ &\quad \times \cos\left(2\pi f_c(kT + t_{p,k}) + \varphi^c_p(kT + t_{p,k})\right) \\ &\approx E^c_p(kT)\cos\left(2\pi f_c kT + 2\pi f_c t_{p,k} + \varphi^c_p(kT)\right) \\ &= E_{p,k}\cos\left(2\pi f_c kT + 2\pi f_c t_{p,k} + \varphi_{p,k}\right) \end{aligned}$$

where the approximation holds because $t_{p,k} \ll T$ (typically tens of microseconds in comparison to tens of milliseconds). Define the phase mismatch

$$\boldsymbol{\theta}_k = 2\pi f_c \boldsymbol{t}_k \quad (14)$$

and use the phasor notation for the complex voltage as $E_{p,k}e^{j(\varphi_{p,k} + \theta_{p,k})}$. The real and imaginary parts of this delayed voltage can be expressed as

$$\tilde{E}^{\mathrm{r}}_{p,k} = E_{p,k}\cos(\varphi_{p,k} + \theta_{p,k}) \approx E^{\mathrm{r}}_{p,k} - E^{\mathrm{i}}_{p,k}\theta_{p,k}, \quad (15)$$

$$\tilde{E}^{\mathrm{i}}_{p,k} = E_{p,k}\sin(\varphi_{p,k} + \theta_{p,k}) \approx E^{\mathrm{i}}_{p,k} - E^{\mathrm{r}}_{p,k}\theta_{p,k} \quad (16)$$

where we have used the standard approximations

$$\sin\theta_{p,k} \approx \theta_{p,k}, \quad \cos\theta_{p,k} \approx 1 \quad (17)$$

which hold for small values of θ_p (typically less than 1 degree, corresponding to 46.3 μs delay at $f_c = 60$ Hz). The delayed currents are detailed in

$$\begin{aligned} \tilde{I}^{\mathrm{r}}_{pq} &= \left(E_p\cos(\varphi_p + \theta_p) - E_q\cos(\varphi_q + \theta_p)\right) g_{pq} \\ &\quad - \left(E_p\sin(\varphi_p + \theta_p) - E_q\sin(\varphi_q + \theta_p)\right) b_{pq} \\ &\quad - B_p E_p \sin(\varphi_p + \theta_p) \\ &\approx E^{\mathrm{r}}_p\left(g_{pq} + b_{pq}\theta_p + B_p\theta_p\right) + E^{\mathrm{r}}_q\left(-g_{pq} - b_{pq}\theta_p\right) \\ &\quad + E^{\mathrm{i}}_p\left(-g_{pq}\theta_p - b_{pq} - B_p\right) + E^{\mathrm{i}}_q\left(g_{pq}\theta_p + b_{pq}\right) \end{aligned} \quad (18)$$

$$\begin{aligned} \tilde{I}^{\mathrm{i}}_{pq} &= \left(E_{p,k}\cos(\varphi_p + \theta_p) - E_q\cos(\varphi_q + \theta_p)\right) b_{pq} \\ &\quad + \left(E_p\sin(\varphi_p + \theta_p) - E_q\sin(\varphi_q + \theta_p)\right) g_{pq} \\ &\quad + B_p E_p \cos(\varphi_p + \theta_p) \\ &\approx E^{\mathrm{r}}_p\left(b_{pq} - g_{pq}\theta_p + B_p\right) \\ &\quad + E^{\mathrm{r}}_q\left(-b_{pq} + g_{pq}\theta_p\right) \\ &\quad + E^{\mathrm{i}}_p\left(-b_{pq}\theta_p + g_{pq} - B_p\theta_p\right) + E^{\mathrm{i}}_q\left(b_{pq}\theta_p - g_{pq}\right). \end{aligned} \quad (19)$$

where we temporarily omitted the subscript k for simplicity of notation. Note that all of the measurements from the PMU installed on a particular bus, namely the voltage and the currents on all of the adjacent branches, are associated with the same phase mismatch θ_p, as they use the same time stamp. Thus, the imperfectly synchronized version of (9) is given by

$$\tilde{\boldsymbol{z}}^p_k = \boldsymbol{H}_p\boldsymbol{s}^p_k + \theta_{p,k}\boldsymbol{G}_p\boldsymbol{s}^p_k \quad (20)$$

where $\boldsymbol{H}_p$ is defined in (10) and $\boldsymbol{G}_p$ is

$$\boldsymbol{G}_p = \begin{bmatrix} -\tilde{\mathbf{I}} & \mathbf{0} & \cdots & \mathbf{0} \\ \boldsymbol{\Xi}_{pq_1} & \tilde{\boldsymbol{\Xi}}_{pq_1} & \cdots & \mathbf{0} \\ \vdots & \vdots & \ddots & \vdots \\ \boldsymbol{\Xi}_{pq_u} & \mathbf{0} & \cdots & \tilde{\boldsymbol{\Xi}}_{pq_u} \end{bmatrix} \quad (21)$$

where

$$\tilde{\mathbf{I}} = \begin{bmatrix} 0 & 1 \\ 1 & 0 \end{bmatrix} \tag{22}$$

$$\boldsymbol{\Xi}_{pq_i} = \begin{bmatrix} b_{pq_i} + B_p & -g_{pq_i} \\ -g_{pq_i} & -b_{pq_i} - B_p \end{bmatrix} \tag{23}$$

$$\tilde{\boldsymbol{\Xi}}_{pq_i} = \begin{bmatrix} -b_{pq_i} & g_{pq_i} \\ g_{pq_i} & b_{pq_i} \end{bmatrix}. \tag{24}$$

Stacking these observations together and padding zeros in appropriate locations in corresponding matrices yields the following bilinear observation model:

$$\boldsymbol{z}_k = \left(\boldsymbol{H} + \sum_{m \in \mathcal{M}} \theta_{m,k} \boldsymbol{G}_m \right) \boldsymbol{s}_k + \boldsymbol{\epsilon}_k \tag{25}$$

where $\boldsymbol{\epsilon}_k$ denotes Gaussian measurement noise following $\mathcal{N}(\mathbf{0}, \boldsymbol{R}_{\epsilon,k})$. In some settings, $\boldsymbol{G}_m$ can be replaced by $\boldsymbol{G}_{m,k}$ to account for time-varying system topology or parameters. It is worth mentioning that, recently, bilinear state estimation approach [27], [28] is also proposed as an alternative to the conventional state estimation based on the well-known Gauss–Newton iterative schemes, where the original nonlinear measurement model is rephrased as two linear models, coupled through a nonlinear change of variables.

B. Dynamic Models for System State and Time Delay

1) System State: Following [18], we adopt a state space linear dynamic model for the system state

$$\boldsymbol{s}_{k+1} = \boldsymbol{A}_{s,k} \boldsymbol{s}_k + \boldsymbol{B}_{s,k} \boldsymbol{u}_{s,k} + \boldsymbol{w}_{s,k}. \tag{26}$$

The matrix $\boldsymbol{A}_{s,k}$ relates the state at the previous time step to the state at the current time step. The matrix $\boldsymbol{B}_{s,k}$ relates the controls and other driving forces $\boldsymbol{u}_{s,k}$ to the state. The random vector $\boldsymbol{w}_{s,k}$ is assumed to be multivariate Gaussian with

$$\boldsymbol{w}_{s,k} \sim \mathcal{N}(\mathbf{0}, \boldsymbol{Q}_{s,k}). \tag{27}$$

The covariance $\boldsymbol{Q}_{s,k}$ can incorporate additional prior information from network topology or SCADA estimation, etc. In a dynamic state estimation scenario, the parameters $\boldsymbol{A}_{s,k}$, $\boldsymbol{B}_{s,k}$, and $\boldsymbol{Q}_{s,k}$ are calculated online through the parameter identification process [29].

2) Time Delay: We assume that the PMUs are jointly synchronized every T_{sync} seconds. Immediately after the synchronization, the delays $\boldsymbol{t}_0$ follow a Gaussian distribution, with

$$\boldsymbol{t}_0 \sim \mathcal{N}(\mathbf{0}, \boldsymbol{R}_{t,0}) \tag{28}$$

where the covariance matrix $\boldsymbol{R}_{t,0}$ depends on the synchronization accuracy of the specific synchronization mechanism employed. Also, depending on the synchronization mechanism, $\boldsymbol{t}_0$ can follow different probability distributions. Between two synchronizations, we assume $\boldsymbol{t}_k$ follows the linear dynamic model

$$\boldsymbol{t}_{k+1} = \boldsymbol{A}_{t,k} \boldsymbol{t}_k + \boldsymbol{B}_{t,k} \boldsymbol{u}_{t,k} + \boldsymbol{w}_{t,k}. \tag{29}$$

The control variable $\boldsymbol{u}_{t,k}$ includes temperature and other control dynamics which affect the time synchronization. The covariance of $\boldsymbol{w}_{t,k}$, $\boldsymbol{Q}_{t,k}$ can be either white Gaussian assuming independent time drifts of different sensors or having topologically based structures associated with advanced distributed synchronization mechanisms. It has been shown in [23] that the clock state of an IEEE 1588 network satisfies a similar linear dynamic model.

III. State Estimation Considering Phase Mismatch

In the previous section we formulated the power grid statistical models. State estimation is the problem of recovering $\boldsymbol{s}_k$ given $\boldsymbol{z}_k, \boldsymbol{z}_{k-1}, \ldots, \boldsymbol{z}_0$. The system state can be estimated using two types of techniques—the static state estimation (SSE) and the dynamic state estimation (DSE) [29]. The SSE estimates the system state at time instant k using measurements for the same instant of time. The most commonly used method for SSE is the weighted least-squares (WLS) method [7]. The DSE depends on physical modeling of the time-varying nature of the power system and employs dynamic state models, e.g., the model defined in (26), where the model parameters are estimated online. The estimation is traditionally obtained using Kalman filtering (KF) [9], [30], [31]. In this paper, we will not discuss system identification. Rather, we assume the system parameters (structures) are known, and propose methods for state estimation based on the static and the dynamic model considering synchronization errors.

We consider a more realistic model defined in (25), (26), and (29). This formulation involves additional nuisance parameters $\boldsymbol{t}_k$ which complicate the inference of $\boldsymbol{s}_k$. The optimal filter solution requires the computation of the posterior distribution of unknown state parameters marginalized over the nuisance parameters and is clearly intractable. Instead, we propose an approximate solution based on joint estimation of both $\boldsymbol{s}_k$ and $\boldsymbol{t}_k$ via two parallel yet coupled Kalman filters under the dynamic model. We also propose an alternating-minimization-based estimation approach under the static model, which is competitive with dynamic filtering in some respects.

A. State Estimation Using Static Model

Static state estimation considers the estimation of $\boldsymbol{s}_k$ given $\boldsymbol{z}_k$. It does not exploit the previous measurements, nor does it assume the dynamical models in (26) and (29). Instead of the dynamic characterization, we assume the time dissynchronizations follow a Gaussian prior distribution

$$\boldsymbol{t}_k \sim \mathcal{N}(\mathbf{0}, \boldsymbol{R}_{t,k}) \tag{30}$$

where $\boldsymbol{R}_{t,k}$ is calculated based on (28) and (29) to yield

$$\boldsymbol{R}_{t,k} = \boldsymbol{R}_{t,0} + \mathrm{mod}\left(k, \frac{1}{T}\right) \boldsymbol{Q}_{t,k}. \tag{31}$$

The covariance $\boldsymbol{R}_{t,k}$ changes with k because the time delay evolves over time following (29), and is reset to $\boldsymbol{R}_{t,0}$ immediately after synchronization. Converting the units, we obtain that the phase mismatch $\boldsymbol{\theta}_k$ follows a simple Gaussian prior $\mathcal{N}(\mathbf{0}, \boldsymbol{R}_{\theta,k})$. We model the states as deterministic unknown variables without any prior distribution. The algorithm can be easily modified to allow additional information, e.g., that provided by existing SCADA estimation. The main advantage of these static simplifications is the robustness to inaccurate state space modeling or inaccurate system identification.

Static state estimation with nuisance phase mismatches is a regularized structured total least squares (STLS) [32] problem, where errors not only exist in the observation vector, but also exist in the data matrix. The errors in the data matrix also exhibits certain structures, and in this case an affine function of the matrices associated with each bus installed with PMUs. Estimating the system state is then a process of finding a solution to the STLS problem, with regularization for the phase mismatch prior. Total least squares (TLS) [33], [34] has a classical closed-form solution based on the singular value decomposition (SVD). However, STLS is an open problem which is still not fully understood. Two possible approaches to STLS are an alternating minimization (AM) method which sequentially solves for the state or the phases independently or a low-rank relaxation technique via nuclear norm minimization [35]. In our setting, the number of measurements is small compared with the number of unknown variables, and the phase mismatch is also relatively small. We found through exploratory experiments that, in this case, the simple AM approach is more preferable than the low-rank relaxation technique. Due to the bilinear structure of (25), the optimal estimator for each of the unknown parameters assuming the other is known has a simple closed-form solution. Thus, we propose the following AM approach.

1) Estimate $\boldsymbol{S}_k$, Assuming $\boldsymbol{\theta}_k$ Is Known: Assuming $\boldsymbol{\theta}_k$ is known, and denoting

$$\boldsymbol{\Phi}(\boldsymbol{\theta}_k) = \left(\boldsymbol{H} + \sum_{m\in\mathcal{M}} \theta_{m,k}\boldsymbol{H}_m\right) \tag{32}$$

we can then write (25) as

$$\boldsymbol{z}_k = \boldsymbol{\Phi}(\boldsymbol{\theta}_k)\boldsymbol{s}_k + \boldsymbol{\epsilon}_k. \tag{33}$$

The maximum-likelihood estimator of $\boldsymbol{s}_k$ is then obtained by solving the weighted least-squares (WLS) problem

$$\hat{\boldsymbol{s}}_k = \arg\min_{\boldsymbol{s}_k} \left(\boldsymbol{z}_k - \boldsymbol{\Phi}(\boldsymbol{\theta}_k)\boldsymbol{s}_k\right)^T \boldsymbol{R}_{\epsilon,k}^{-1}\left(\boldsymbol{z}_k - \boldsymbol{\Phi}(\boldsymbol{\theta}_k)\boldsymbol{s}_k\right). \tag{34}$$

The closed-form solution to (34) is

$$\hat{\boldsymbol{s}}_k = \left(\boldsymbol{\Phi}(\boldsymbol{\theta}_k)^T\boldsymbol{R}_{\epsilon,k}^{-1}\boldsymbol{\Phi}(\boldsymbol{\theta}_k)\right)^{-1}\boldsymbol{\Phi}(\boldsymbol{\theta}_k)^T\boldsymbol{R}_{\epsilon,k}^{-1}\boldsymbol{z}_k. \tag{35}$$

In this step, it is also possible to include the state estimation from the SCADA system, as prior information. Then, we can assume a Gaussian prior distribution of the system state

$$\boldsymbol{s}_k \sim \mathcal{N}(\check{\boldsymbol{s}}_k, \check{\boldsymbol{R}}_{s,k}) \tag{36}$$

where $\check{\boldsymbol{s}}_k$ and $\check{\boldsymbol{R}}_{s,k}$ denote the system state and covariance estimated using the SCADA system. With this prior information, we can then replace the maximum-likelihood estimator (34) with a maximum *a posteriori* (MAP) estimator to estimate system state $\boldsymbol{s}_k$.

2) Estimate $\boldsymbol{\theta}_k$, Assuming $\boldsymbol{S}_k$ Is Known: Assuming $\boldsymbol{s}_k$ is known from (34), we estimate the phase mismatch $\boldsymbol{\theta}_k$. Let $\boldsymbol{\psi}_m(\boldsymbol{s}_k) = \boldsymbol{H}_m\boldsymbol{s}_k$ and $\boldsymbol{\Psi}(\boldsymbol{s}_k) = [\ldots,\boldsymbol{\psi}_m(\boldsymbol{s}_k),\ldots]$, where $m \in \mathcal{M}$. We can then write (25) as

$$\boldsymbol{z}_k = \boldsymbol{H}\boldsymbol{s}_k + \boldsymbol{\Psi}(\boldsymbol{s}_k)\boldsymbol{\theta} + \boldsymbol{\epsilon}_k. \tag{37}$$

The MAP estimator of $\boldsymbol{\theta}_k$ is then

$$\begin{aligned}\hat{\boldsymbol{\theta}}_k = \arg\min_{\boldsymbol{\theta}_k} &\left(\boldsymbol{z}_k - \boldsymbol{H}\boldsymbol{s}_k - \boldsymbol{\Psi}(\boldsymbol{s}_k)\boldsymbol{\theta}_k\right)\boldsymbol{R}_{\epsilon,k}^{-1} \\ &\times \left(\boldsymbol{z}_k - \boldsymbol{H}\boldsymbol{s}_k - \boldsymbol{\Psi}(\boldsymbol{s}_k)\boldsymbol{\theta}_k\right) + \boldsymbol{\theta}_k^T\boldsymbol{R}_{\theta,k}^{-1}\boldsymbol{\theta}_k\end{aligned} \tag{38}$$

and the closed-form solution is

$$\hat{\boldsymbol{\theta}}_k = \left(\boldsymbol{\Psi}(\boldsymbol{s}_k)^T\boldsymbol{R}_{\epsilon,k}^{-1}\boldsymbol{\Psi}(\boldsymbol{s}_k) + \boldsymbol{R}_{\theta,k}^{-1}\right)^{-1}\boldsymbol{\Psi}(\boldsymbol{\theta}_k)^T\boldsymbol{R}_{\epsilon,k}^{-1}(\boldsymbol{z}_k - \boldsymbol{H}\boldsymbol{s}_k). \tag{39}$$

3) Alternating Algorithm for Joint Estimation: The estimation algorithm iterates between the two steps described above and solves for the state of the system. The alternating algorithm is described in Algorithm 1.

Algorithm 1 AM Approach for Static State Estimation Considering PMU Phase Mismatch.

Data: observations $\boldsymbol{z}_k$.

Result: state estimation $\boldsymbol{s}_k$.

begin

  initialize $\boldsymbol{\theta}_k$;

  repeat

    update $\boldsymbol{s}_k$ using **(35)**;

    update $\boldsymbol{\theta}_k$ using **(39)**;

  until convergence or max iterations achieved;

end

A possible drawback to Algorithm 1 is that multiple iterations have to be executed for each estimation. However, under the assumption that the phase mismatch changes slowly, the phase mismatch from a previous time point can be used to “warm start” the current estimation, thus reducing the number of iterations.

B. State Estimation Using Dynamic Model

Here, we consider the case of state estimation using the dynamic models (26) and (29). Kalman filtering is widely used in online state estimation and is employed for power system state estimation problems [9], [30], [31]. For a perfectly synchronized linear dynamic model with white Gaussian noise, the Kalman filter is known to be optimal. Our mismatched model is bilinear and more difficult. Two vectors of parameters has to be estimated jointly, i.e., the phase mismatch $\boldsymbol{\theta}_k$ and the system state $\boldsymbol{s}_k$.

Based on the system dynamics and the measurement model, different approximate methods could potentially be used to dynamically estimate the state $\boldsymbol{s}_k$ and phase mismatch $\boldsymbol{\theta}_k$, including total Kalman filtering [36], recursive total least squares [37], etc. Our experiments suggest that parallel Kalman filtering (PKF) [26] is simple to use and produces accurate estimation results.

The idea of the PKF [26] was from the theory of two-player dynamic game theory [38]. The solution of the game, i.e., the equilibrium, is such that each player selects its best strategy corresponding to the other player's strategy. In the context of our problem, we can consider the bilinear state estimation problem as two players, with strategy sets to be the estimate of the system state and the estimate of the phase mismatch. The cost function of each player is the estimation error. Therefore, the solution of the game should satisfy

$$\hat{\boldsymbol{s}}^*_{k|k} = \arg\min_{\hat{\boldsymbol{s}}_{k|k}} u_s\left(\hat{\boldsymbol{s}}_{k|k}, \hat{\boldsymbol{\theta}}^*_{k|k}\right) \tag{40}$$

$$\hat{\boldsymbol{\theta}}^*_{k|k} = \arg\min_{\hat{\boldsymbol{\theta}}_{k|k}} u_\theta\left(\hat{\boldsymbol{s}}^*_{k|k}, \hat{\boldsymbol{\theta}}_{k|k}\right). \tag{41}$$

In practice, we use the "optimal predicted estimates" $\hat{\boldsymbol{\theta}}^*_{k|k-1}$ and $\hat{\boldsymbol{s}}^*_{k|k-1}$ instead of $\hat{\boldsymbol{\theta}}^*_{k|k}$ and $\hat{\boldsymbol{s}}^*_{k|k}$ to parallel the two filters. In this way, we reformulated the original problem into two interlaced estimation problems on two linear time-varying systems. To simplify the notations, we define

$$\boldsymbol{C}_\theta(\boldsymbol{\theta}_k) = \sum_{m\in\mathcal{M}} \theta_{m,k}\boldsymbol{G}_{m,k} \tag{42}$$

$$\boldsymbol{C}_s(\boldsymbol{s}_k) = [\ldots, \boldsymbol{G}_{m,k}\boldsymbol{s}_k, \ldots], \qquad \text{where } m \in \mathcal{M} \tag{43}$$

and therefore the original model (25) can be rewritten as

$$\boldsymbol{z}_k = \boldsymbol{H}\boldsymbol{s}_k + \boldsymbol{C}_\theta(\boldsymbol{\theta}_k)\boldsymbol{s}_k + \boldsymbol{\epsilon}_k \tag{44}$$

$$\boldsymbol{z}_k = \boldsymbol{H}\boldsymbol{s}_k + \boldsymbol{C}_s(\boldsymbol{s}_k)\boldsymbol{\theta}_k + \boldsymbol{\epsilon}_k. \tag{45}$$

We then decompose the original system into two subsystems. The subsystem for system state can then be characterized by (26) and (44), whereas the subsystem for phase mismatch can be characterized by (29) and (45). Note that the unit in (29) needs to be converted into the unit of phase, and we use $\boldsymbol{A}_{\theta,k}, \boldsymbol{B}_{\theta,k}$ and $\boldsymbol{u}_{\theta,k}$ to denote parameters and control variables corresponding to the phase mismatch.

1) State and Phase Mismatch Estimation: Based on the two subsystem models, we can couple two Kalman filters—one for state estimation and one for phase mismatch estimation. First, the predicted estimates $\hat{\boldsymbol{\theta}}_{k|k-1}$ and $\hat{\boldsymbol{s}}_{k|k-1}$ will be calculated. When a measurement is received, the two filters updates the estimates accordingly in parallel. The updated estimate will be used for prediction in the next time instant. The formulas for the predictions and updates are listed below, where we use superscripts s and θ to distinguish covariance matrices for the state and phase mismatch, respectively.

Prediction:

$$\begin{aligned}
\hat{\boldsymbol{s}}_{k|k-1} &= \boldsymbol{A}_{s,k}\hat{\boldsymbol{s}}_{k-1|k-1} + \boldsymbol{B}_{s,k}\boldsymbol{u}_{s,k}\\
\hat{\boldsymbol{\theta}}_{k|k-1} &= \boldsymbol{A}_{\theta,k}\hat{\boldsymbol{\theta}}_{k-1|k-1} + \boldsymbol{B}_{\theta,k}\boldsymbol{u}_{\theta,k}\\
\boldsymbol{P}^{(s)}_{k|k-1} &= \boldsymbol{A}_{s,k}\boldsymbol{P}^{(s)}_{k-1|k-1}\boldsymbol{A}^T_{s,k} + \boldsymbol{Q}_{s,k}\\
\boldsymbol{P}^{(\theta)}_{k|k-1} &= \boldsymbol{A}_{\theta,k}\boldsymbol{P}^{(\theta)}_{k-1|k-1}\boldsymbol{A}^T_{\theta,k} + \boldsymbol{Q}_{\theta,k}.
\end{aligned}$$

Update:

$$\begin{aligned}
\boldsymbol{K}^{(s)}_k =& \boldsymbol{P}^{(s)}_{k|k-1}\left(\boldsymbol{H} + \boldsymbol{C}_\theta(\hat{\boldsymbol{\theta}}_{k|k-1})\right)^T\\
&\times\left(\left(\boldsymbol{H}+\boldsymbol{C}_\theta(\hat{\boldsymbol{\theta}}_{k|k-1})\right)\boldsymbol{P}^{(s)}_{k|k-1}\left(\boldsymbol{H}+\boldsymbol{C}_\theta(\hat{\boldsymbol{\theta}}_{k|k-1})\right)^T\right.\\
&\left.+\boldsymbol{R}_{\epsilon,k}\right)^{-1}\\
\boldsymbol{K}^{(\theta)}_k =& \boldsymbol{P}^{(\theta)}_{k|k-1}\boldsymbol{C}_s(\hat{\boldsymbol{s}}_{k|k-1})^T\\
&\left(\boldsymbol{C}_s(\hat{\boldsymbol{s}}_{k|k-1})\boldsymbol{P}^{(s)}_{k|k-1}\boldsymbol{C}_s(\hat{\boldsymbol{s}}_{k|k-1})^T + \boldsymbol{R}_{\epsilon,k}\right)^{-1}\\
\boldsymbol{P}^{(s)}_{k|k} =& \boldsymbol{P}^{(s)}_{k|k-1} - \boldsymbol{K}^{(s)}_k\left(\boldsymbol{H} + \boldsymbol{C}_\theta(\hat{\boldsymbol{\theta}}_{k|k-1})\right)\boldsymbol{P}^{(s)}_{k|k-1}\\
\boldsymbol{P}^{(\theta)}_{k|k} =& \boldsymbol{P}^{(\theta)}_{k|k-1} - \boldsymbol{K}^{(\theta)}_k\left(\boldsymbol{H} + \boldsymbol{C}_s(\hat{\boldsymbol{s}}_{k|k-1})\right)\boldsymbol{P}^{(\theta)}_{k|k-1}\\
\hat{\boldsymbol{s}}_{k|k} =& \hat{\boldsymbol{s}}_{k|k-1} + \boldsymbol{K}^{(s)}_k\left(\boldsymbol{z}_k - \left(\boldsymbol{H} + \boldsymbol{C}_\theta(\hat{\boldsymbol{\theta}}_{k|k-1})\right)\hat{\boldsymbol{s}}_{k|k-1}\right)\\
\hat{\boldsymbol{\theta}}_{k|k} =& \hat{\boldsymbol{\theta}}_{k|k-1} + \boldsymbol{K}^{(\theta)}_k\left(\boldsymbol{z}_k - \left(\boldsymbol{H}\hat{\boldsymbol{s}}_{k|k-1} + \boldsymbol{C}_s(\hat{\boldsymbol{s}}_{k|k-1})\hat{\boldsymbol{\theta}}_{k|k-1}\right)\right).
\end{aligned}$$

2) Synchronization Model: Our proposed phase-mismatch model assumes that the PMUs are synchronized every few seconds. This needs to be taken into consideration when coupling the two Kalman filters. For estimation of the phase mismatch, the matrix $\boldsymbol{P}^{(\theta)}_{k,k}$ has to be reset at the time of synchronization. In addition, since we are coupling this Kalman filter with the filter for state estimation, the state estimate also has to be changed at the time of synchronization. A reasonable strategy is to assume zero phase mismatch at the time of synchronization, as the phase mismatch is often very small immediately after synchronization. Then, we directly use the weighted least-squares estimate without considering phase mismatch to reset the filter for state estimation. Due to the Gaussian linear model, all of the prediction and update steps are closed-form and computationally efficient.

IV. Numerical Examples

Here, we use numerical examples to illustrate the improvement achieved by the proposed state estimation algorithms compared with commonly used methods. We also illustrate the effect of the number of PMUs installed, the time synchronization parameters, and the synchronization interval on the estimation performance.

A. General Setup

We assume the PMUs reports 30 times per second and are synchronized every second unless otherwise specified. At time of synchronization, the time delay follows (28), and, between consecutive synchronization, the time delay follows the linear dynamic model (29). Without loss of generality, we assume the synchronization of different PMUs are independent, and therefore $\boldsymbol{R}_{t,0} = \sigma^2_{t,0}\mathbf{I}$ and $\boldsymbol{Q}_{t,k} = \sigma^2_{t,k}\mathbf{I}$. This assumption is not necessary and is only for ease and clarity of the performance evaluation. In the numerical examples, we set $\sigma_{t,0} = \sigma_{t,k} = 5\ \mu$s except in the example where we illustrate the effect of synchronization accuracy on the estimation performance.

The power system is quasi-static, and the change of states is relatively slow comparing with the high PMU reporting rate. Therefore, in the simulation, we select $\boldsymbol{Q}_{s,k} = \sigma_{s,k}\mathbf{I}$, with $\sigma_{s,k} = 10^{-3}$p.u.[29]. We set $\boldsymbol{A}_{s,k}$ to be identity matrix [18] and

This article has been accepted for inclusion in a future issue of this journal. Content is final as presented, with the exception of pagination.

TABLE I
PMU LOCATIONS FOR DIFFERENT TEST SYSTEMS

# of Buses	# of PMUs	Indices of Buses with PMUs
14	4	2, 6, 7, 9
	6	2, 4, 6, 7, 9, 13
30	10	1, 7, 9, 10, 12, 18, 24, 25, 27, 28
	16	3, 4, 5, 7, 10, 11, 12, 17, 19, 22, 24, 25, 26, 28, 29, 30
57	17	1, 4, 6, 13, 20, 22, 25, 27, 29, 32, 36, 39, 41, 45, 47, 51, 54
	28	1, 3, 4, 6, 9, 12, 20, 22, 24, 27, 29, 30, 32, 34, 36, 38, 39, 41, 43, 44, 45, 46, 48, 51, 52, 53, 54, 56
118	32	3, 7, 9, 11, 12, 17, 21, 25, 28, 34, 37, 41, 45, 49, 53, 56, 62, 63, 68, 70, 71, 76, 79, 85, 86, 89, 92, 96, 100, 105, 110, 114
	54	2, 5, 8, 10, 12, 15, 17, 21, 22, 25, 26, 29, 31, 36, 37, 41, 42, 43, 44, 46, 53, 54, 56, 57, 58, 62, 64, 67, 68, 69, 70, 71, 73, 75, 77, 79, 80, 83, 85, 87, 90, 91, 94, 100, 101, 102, 105, 107, 110, 112, 114, 115, 116, 118

$\boldsymbol{B}_{s,k}$ to be zero matrix in the simulations. This specific choice of parameter does not affect the generality of our algorithm. As we mentioned before, these system parameters are estimated online through system identification in the dynamic state estimation scenario. The initial state $\boldsymbol{s}_0$ is defined via its magnitude $\boldsymbol{E}_0$ and angle $\boldsymbol{\varphi}_0$ and generated from the following distributions:

$$\begin{aligned} \boldsymbol{E}_0 &\sim \mathcal{N}(\mathbf{1}, 0.05^2\mathbf{I}) \quad \text{p.u.} \\ \boldsymbol{\varphi}_0 &\sim \mathcal{U}(\mathbf{0}, \mathbf{2}\pi) \text{ rad.} \end{aligned} \tag{46}$$

These initial distributions are used for data generation purposes only and are not exploited by the estimation methods. The measurement noise is assumed to be i.i.d. Gaussian, with $\boldsymbol{R}_{\epsilon,k} = \sigma_\epsilon^2\mathbf{I}$, and $\sigma_\epsilon = 5 \times 10^{-3}$ p.u.

We test the performance of our algorithms on the IEEE 14-, 30-, 57-, and 118-bus systems. For each test system, we consider two scenarios—one with the minimum number of PMUs installed for full (topological) observation and one with redundant observations on selected buses. In this numerical example, the placement of the minimum number of PMUs for the first scenario is obtained using the method proposed in [17]. For the second scenario, the buses with redundant observations are randomly selected. In reality, we can assign more redundant observations on more important buses. We include the PMU placement profile for different test cases and different scenarios in Table I.

We use the root mean squared error (RMSE) as the performance measure. For each time point, we calculate the RMSE of the magnitude and angle of the bus voltages and then average the RMSE over all the time points. In each test, we execute 20 Monte Carlo simulations with 600 data points (equivalent to 20 s of data).

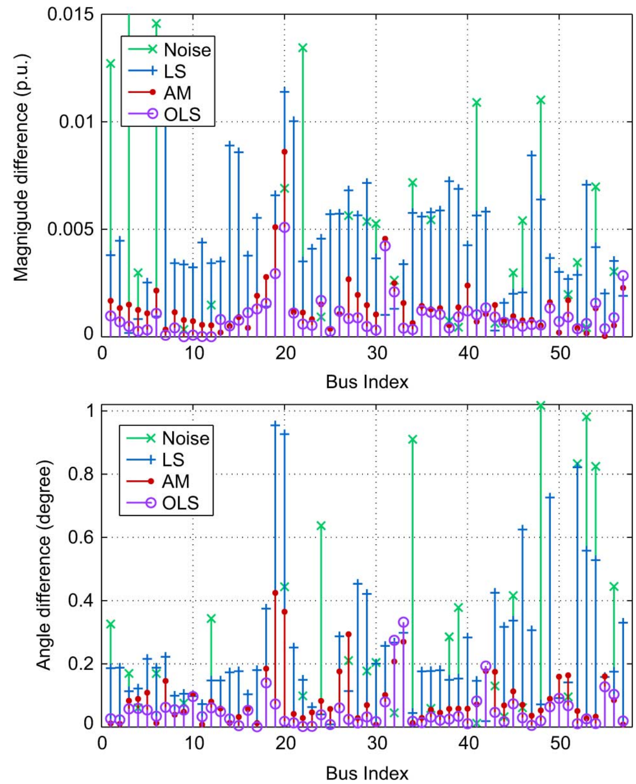

Fig. 3. Comparison of state estimation results at one time point using AM, LS, and OLS on the IEEE 57-bus system with 28 PMUs.

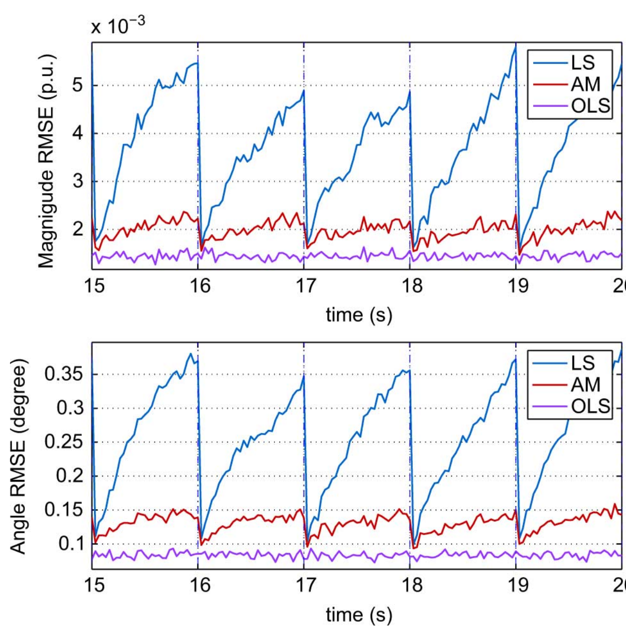

Fig. 4. Comparison of state estimation results for 5 s using AM, LS, and OLS on IEEE 57-bus system with 28 PMUs.

B. Example Using Static Models

We first consider state estimation using static models, where the state at time point k is estimated based on measurements at the same time point only and does not consider system dynamics. We compare our AM method with the traditional least-squares (LS) estimation.

Under the general setup, we run Algorithm 1 for static state estimation. The estimation error at one time point is shown in Fig. 3, where we compare the absolute magnitude and angle difference for the estimation of each bus state with the actual observed noise. We also include an "oracle case" (OLS) for comparison. The oracle estimatoin is obtained by assuming perfect knowledge of the phase mismatch, and using a simple LS to estimate the states. Note that in the model we used real and imaginary parts of the complex-valued states and measurements. Here

TABLE II
RMSE OF ESTIMATION USING STATIC MODELS ON DIFFERENT TEST SYSTEMS USING LS, AM, AND OLS

# of Buses N	# of PMUs M	Least Squares		Alternating Minimization		Oracle		Improvement	
		Magnitude (p.u.)	Angle (degrees)	Magnitude (p.u.)	Angle (degrees)	Magnitude (p.u.)	Angle (degrees)	Magnitude (percentage)	Angle (percentage)
14	4	5.020e-03	0.2827	2.976e-03	0.1781	1.454e-03	0.0832	40.72%	36.99%
	6	4.946e-03	0.2488	2.251e-03	0.1323	1.016e-03	0.0586	54.49%	46.81%
30	10	4.467e-03	0.2788	4.187e-03	0.2432	2.998e-03	0.1719	6.26%	12.75%
	16	2.918e-03	0.2202	2.180e-03	0.1402	1.640e-03	0.0941	25.29%	36.36%
57	17	5.865e-03	0.3519	5.718e-03	0.3320	4.219e-03	0.2416	2.50%	5.67%
	28	3.711e-03	0.2648	2.021e-03	0.1331	1.447e-03	0.0832	45.55%	49.75%
118	32	6.943e-03	0.4709	3.691e-03	0.2198	2.223e-03	0.1278	46.84%	53.31%
	54	5.875e-03	0.3864	1.933e-03	0.1180	7.257e-04	0.0419	67.09%	69.45%

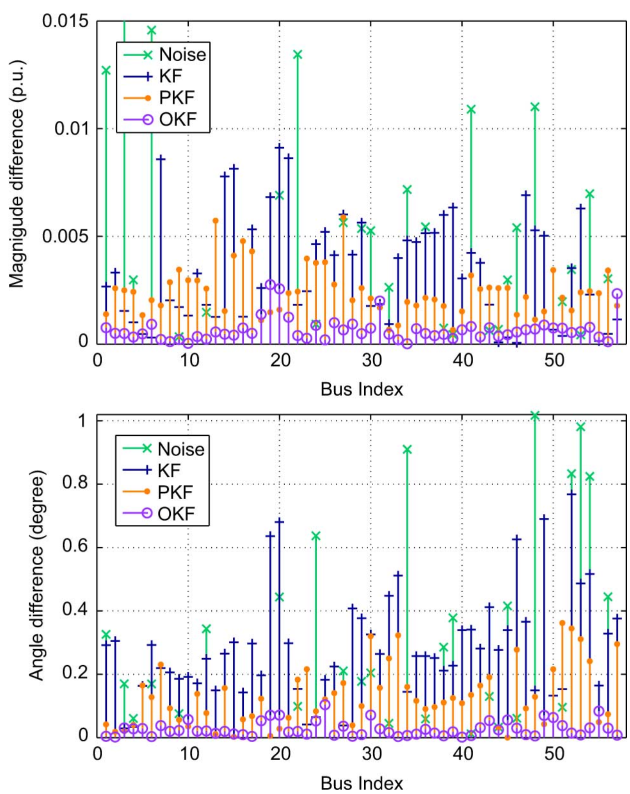

Fig. 5. Comparison of state estimation results at one time point using KF, PKF, and OPK on the IEEE 57-bus system with 28 PMUs.

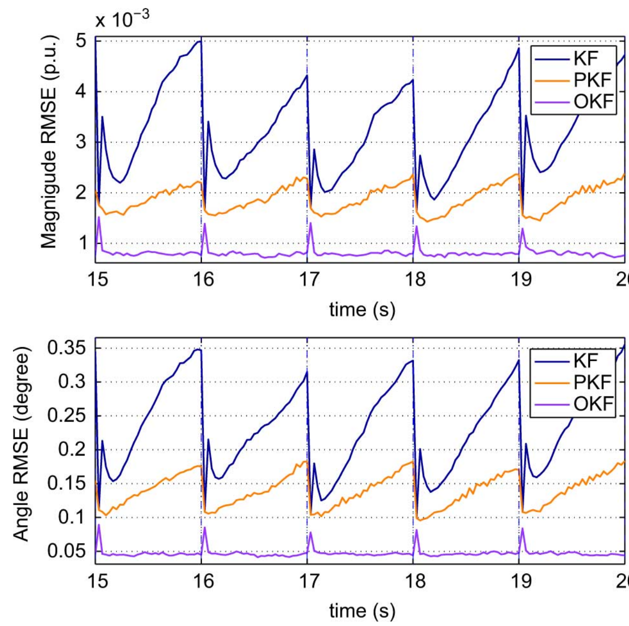

Fig. 6. Comparison of state estimation results for 5 s using KF, PKF, and OPK on IEEE 57-bus system with 28 PMUs.

we convert them into magnitudes and angles for easier comparison. We also compare the magnitude and angle RMSE for five consecutive seconds (150 samples) in Fig. 4. When considering phase mismatch in the estimation model, and employing the AM algorithm for state estimation, we observe that the estimation errors in both magnitude and angle are reduced, and the errors from AM are comparable to the oracle case.

We show the RMSE of LS, AM, and OLS in all the test scenarios in Table II. The improvement is defined by $(1-\mathrm{RMSE}_{\mathrm{AM}}/\mathrm{RMSE}_{\mathrm{LS}}) \times 100\%$, which indicates the reduction in RMSE when using AM instead of LS. We observe that in all the test scenarios, AM provides more accurate estimate than LS. The improvement is more significant when there are redundant observations provided by additional PMUs, as these provide a more accurate estimate of PMU phase mismatch. We also observe that when the number of PMUs increases, the AM estimation is closer to the oracle case.

C. Example Using Dynamic Models

We then consider the state estimation using dynamic models, where the state at time point k is estimated using all of the measurements until the kth time point. We compare our PKF method with the traditional KF and the oracle case (OKF). The OKF assumes perfect knowledge of phase mismatch and employs Kalman filtering for state estimation.

The state estimation error at one time point is shown in Fig. 5 and for five consecutive seconds shown in Fig. 6. The figures indicate that, by using PKF, we can accurately estimate the phase mismatch, which significantly increase the estimation accuracy of system state. Table III compares the RMSE using KF, PKF, and OKF in different test scenarios. Similar to the static case, the improvement is defined by $(1 - \mathrm{RMSE}_{\mathrm{PKF}}/\mathrm{RMSE}_{\mathrm{KF}}) \times 100\%$. We observe similar improvements as in the static case.

D. Comparison Between AM and PKF

In this subsection we compare the performance of AM and PKF. The performance of these two algorithms can be compared using Tables II and III, as the two methods were tested using the same setup and data. We also show a comparison of the RMSE of the two methods in five consecutive seconds in Fig. 7. As can be seen from the tables and the figure, generally PKF provides

TABLE III
RMSE OF ESTIMATION USING DYNAMIC MODELS ON DIFFERENT TEST SYSTEMS USING TRADITIONAL KF, PKF, AND OKF

# of Buses N	# of PMUs M	Kalman Filter		Parallel Kalman Filter		Oracle		Improvement	
		Magnitude (p.u.)	Angle (degrees)	Magnitude (p.u.)	Angle (degrees)	Magnitude (p.u.)	Angle (degrees)	Magnitude (percentage)	Angle (percentage)
14	4	4.774e-03	0.2725	2.840e-03	0.1590	8.723e-04	0.0505	40.51%	41.63%
	6	4.655e-03	0.2336	2.720e-03	0.1395	7.000e-04	0.0402	41.57%	40.25%
30	10	3.061e-03	0.2048	2.563e-03	0.1630	1.287e-03	0.0732	16.29%	20.43%
	16	2.410e-03	0.1928	1.758e-03	0.1269	9.057e-04	0.0518	27.03%	34.17%
57	17	3.751e-03	0.2389	3.613e-03	0.2170	1.607e-03	0.0930	3.67%	9.19%
	28	3.200e-03	0.2375	1.868e-03	0.1392	8.163e-04	0.0471	41.64%	41.39%
118	32	6.010e-03	0.4127	3.277e-03	0.2098	9.473e-04	0.0547	45.47%	49.16%
	54	5.546e-03	0.3640	3.117e-03	0.2037	5.111e-04	0.0296	43.80%	44.02%

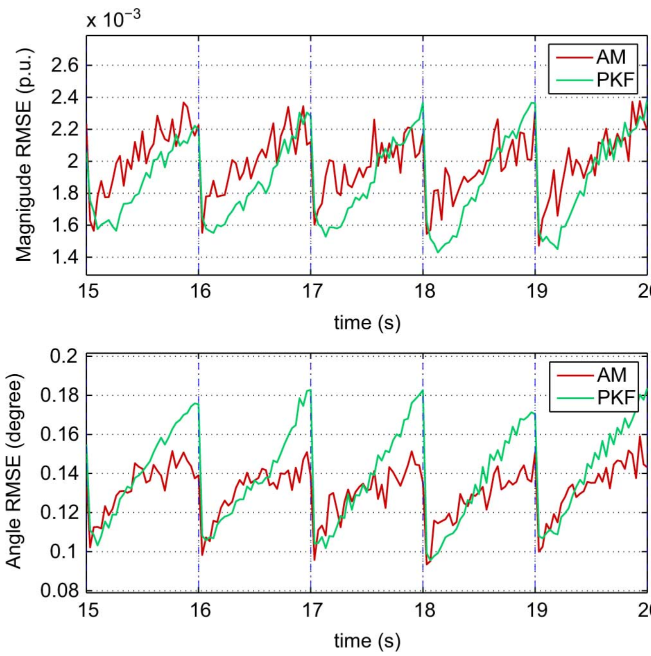

Fig. 7. Comparison of estimation results using AM and PKF on IEEE 57-bus system with 28 PMUs.

slightly better estimation results than the AM, as it employs the dynamic models of the system. In addition, PKF is computationally more efficient than AM, as it does not require iterative methods for the estimation at each time point. However, the AM does not make assumptions on the dynamics of the system or the phase mismatch, and does not rely on an accurate system identification process. Therefore, the AM is more robust to inaccurate system identification than the PKF.

E. Effect of Number of PMUs

The number of installed PMUs affect the estimation performance. In this experiment, we use a numerical example to show how the estimation errors depends on the number of PMUs. Here, we compare AM and LS. The results using KF and PKF are similar.

We assume the installed PMUs have the same synchronization accuracy, with $\sigma_{t,k} = 5\ \mu$s. The optimal PMU placement involves minimizing the estimation error and other cost functions, and is beyond the scope of this paper. We will investigate this problem in our next work. In this work, we employ an *ad hoc* approach to determine PMU placement for illustration purposes. Let $\mathcal{M}$ denote the set of buses with PMUs. We first select

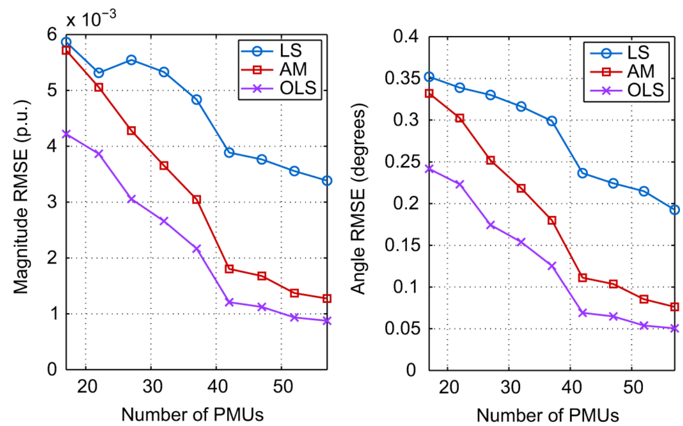

Fig. 8. RMSE as a function of number of PMUs installed on IEEE 57-bus system.

the minimum set of PMUs for full observation using the method from [17], and assign this minimum set to $\mathcal{M}$. Then, we rank the remaining buses in decreasing order according to the number of their adjacent buses and add new buses to $\mathcal{M}$ following this order. In this way, buses with more adjacent buses have higher priority of being selected for PMU installation.

In Fig. 8, we plot the estimation error as a function of the number of PMUs installed. We observe that the performance improves as more PMUs are installed. The improvement is more significant when more PMUs are installed, in which case the difference between our method and the oracle also decreases. This observation provides an intuition for optimal placement of PMUs, which we will analyze in our future work. Note that, in this example, we set the PMU time synchronization specifications $\sigma_{t,k}$ to be the same for all PMUs. In practice, these specifications can be different, adding another design variable to the optimal PMU placement problem.

F. Effect of Synchronization Specifications

We finally illustrate the effect of PMU synchronization specifications on the estimation results. The synchronization specifications includes two aspects—the synchronization accuracy $\sigma_{t,k}$, and the time interval between two consecutive synchronization.

In Fig. 9, we plot the estimation error as a function of $\sigma_{t,k}$ on the IEEE 57-bus system with 28 PMUs installed. We observe that, as $\sigma_{t,k}$ increases, the error also increases. However, since in our proposed methods we estimate the phase mismatch, the error of our proposed method is always lower than that of the

This article has been accepted for inclusion in a future issue of this journal. Content is final as presented, with the exception of pagination.

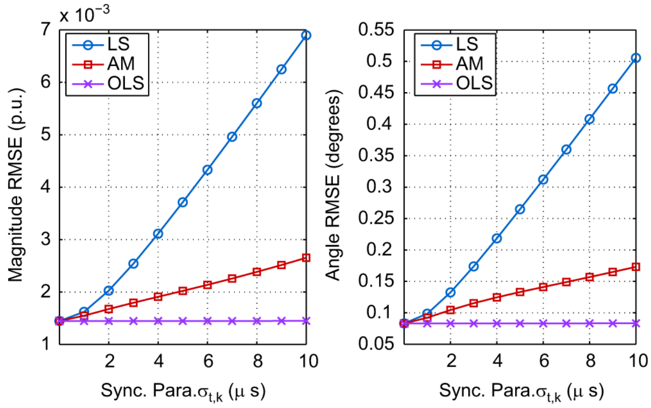

Fig. 9. RMSE as a function of $\sigma_{t,k}$ on IEEE 57-bus system with 28 PMUs.

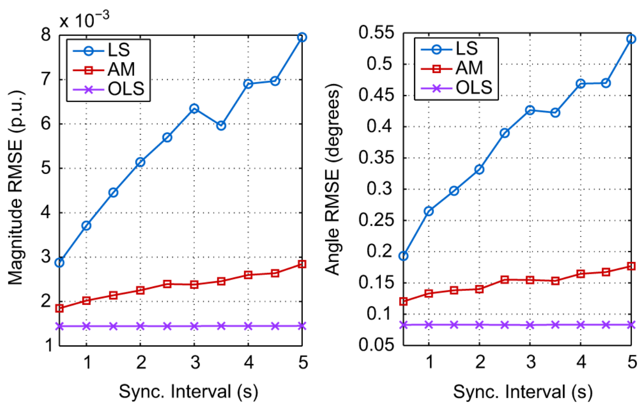

Fig. 10. RMSE as a function of the time interval between consecutive synchronization on IEEE 57-bus system.

LS approach. The improvement is more significant when $\sigma_{t,k}$ is large. The error of the oracle case does not change as the perfect phase mismatch is always assumed known.

Finally, we illustrate the impact of synchronization intervals on the estimation performance. Different synchronization mechanism has different synchronization intervals. For example, PMUs using a GPS clock are synchronized every 1 s, whereas, according to the IEEE 1588 standard, the clocks are synchronized every few seconds. In Fig. 10, we show the estimation performance when the synchronization interval changes. We observe that, as the time interval between consecutive synchronization increases, the estimation error also increases. However, using our methods, the increase in RMSE is much slower. We also performed experiments using KF and PKF, and the results are similar.

V. Conclusion

In this paper, we proposed a model for power system state estimation using PMUs with imperfect synchronization. We then proposed estimation algorithms using the static and dynamic models, with different assumptions. For estimation using the static models, we proposed to use AM to jointly estimate the phase mismatch of PMUs and the state of the power system. This approach does not rely on an accurate dynamic model for the state and phase mismatch, which is the main advantage of this approach over the dynamic counterpart. For estimation using the dynamic models, we proposed to couple two Kalman filters to estimate the phase mismatch and system state in parallel. Given a proper dynamic model for the system, this approach is more preferable as no iterations are required. Numerical examples showed that our methods significantly improve the estimation performance compared with traditional least-squares and Kalman filtering methods when the PMUs are not perfectly synchronized. The PKF in general performs slightly better then the AM. We also illustrated the effect of PMU numbers and PMU synchronization on state estimation, and showed that when a sufficient number of PMUs are installed, the phase mismatch can be largely compensated using signal processing techniques, which encourages large scale deployment of imperfect PMUs. In addition, we showed that the estimation accuracy degrades slowly when the time interval between two synchronization increases when using our methods, which potentially encourages the use of alternative synchronization mechanism with longer synchronization intervals.

In our future work, we will derive analytical performance bounds on the estimation errors, and consider optimal PMU placement problems based on our proposed phase mismatch model. In addition, we will continue to investigate and develop robust algorithms for power system state estimation.

Acknowledgment

The authors would like to thank Prof. D. Dolev and Dr. T. Anker for introducing them to the IEEE 1588 standard.

References

[1] J. D. L. Ree, V. Centeno, J. Thorp, and A. Phadke, "Synchronized phasor measurement applications in power systems," *IEEE Trans. Smart Grid*, vol. 1, no. 1, pp. 20–27, Jun. 2010.
[2] F. Schweppe and E. Handschin, "Static state estimation in electric power systems," *Proc. IEEE*, vol. 62, no. 7, pp. 972–982, Aug. 1974.
[3] O. Smith, "Power system state estimation," *IEEE Trans. Power App. Syst.*, vol. PAS-89, no. 3, pp. 363–379, Mar. 1970.
[4] A. Debs and R. Larson, "A dynamic estimator for tracking the state of a power system," *IEEE Trans. Power App. Syst.*, vol. PAS-89, no. 7, pp. 1670–1678, Sep. 1970.
[5] A. Monticelli, *State Estimation in Electric Power Systems: A Generalized Approach*. New York, NY, USA: Springer, 1999.
[6] K.-R. Shih and S.-J. Huang, "Application of a robust algorithm for dynamic state estimation of a power system," *IEEE Trans. Power Syst.*, vol. 17, no. 1, pp. 141–147, Feb. 2002.
[7] A. Abur and A. G. Expósito, *Power System State Estimation: Theory and Implementation*. New York, NY, USA: Marcel Dekker, 2004.
[8] M. Zhou, V. Centeno, J. Thorp, and A. Phadke, "An alternative for including phasor measurements in state estimators," *IEEE Trans. Power Syst.*, vol. 21, no. 4, pp. 1930–1937, Nov. 2006.
[9] A. Jain and N. Shivakumar, "Impact of PMU in dynamic state estimation of power systems," in *Proc. 40th North Amer. Power Symp.*, Sep. 2008, pp. 1–8.
[10] S. Chakrabarti and E. Kyriakides, "PMU measurement uncertainty considerations in WLS state estimation," *IEEE Trans. Power Syst.*, vol. 24, no. 2, pp. 1062–1071, Apr. 2012.
[11] E. Farantatos, G. Stefopoulos, G. Cokkinides, and A. Meliopoulos, "Pmu-based dynamic state estimation for electric power systems," in *Proc. Power Energy Soc. General Meeting*, Jul. 2009, pp. 1–8.
[12] L. Vanfretti, J. H. Chow, S. Sarawgi, and B. Fardanesh, "A phasor-data based state estimation incorporating phase bias correction," *IEEE Trans. Power Syst.*, vol. 26, no. 1, pp. 111–119, Feb. 2011.
[13] V. Kekatos and G. B. Giannakis, "Distributed robust power system state estimation," *IEEE Trans. Power Syst.*, vol. 28, no. 2, pp. 1617–1626, May 2013.
[14] Y.-F. Huang, S. Werner, J. Huang, N. Kashyap, and V. Gupta, "State estimation in electric power grids: Meeting new challenges presented by the requirements of the future grid," *IEEE Signal Process. Mag.*, vol. 29, no. 5, pp. 33–43, Sep. 2012.

[15] D. G. Hart, D. Uy, V. Gharpure, D. Novosel, D. Karlsson, and M. Kaba, "PMUs—A new approach to power network monitoring." ABB, 2001.

[16] V. Kekatos, G. B. Giannakis, and B. Wollenberg, "Optimal placement of phasor measurement units via convex relaxation," *IEEE trans. Power Syst.*, vol. 27, no. 3, pp. 1521–1530, Aug. 2012.

[17] B. Gou, "Generalized integer linear programming formulation for optimal PMU placement," *IEEE Trans. Power Syst.*, vol. 23, no. 3, pp. 1099–1104, Aug. 2008.

[18] J. Zhang, G. Welch, and G. Bishop, "Observability and estimation uncertainty analysis for PMU placement alternatives," in *Proc. North Amer. Power Symp.*, Sep. 2010, pp. 1–8.

[19] KEMA, Inc., United Telecom Council, , "Substation Communications: Enabler of automation/an assessment of communications technologies," 2006.

[20] M. Begovic, D. Novosel, and B. Djokic, "Issues related to the implementation of synchrophasor measurements," in *Proc. 41st Annu. Hawaii Int. Conf. Syst Sci.*, 2008, p. 164.

[21] A. P. Meliopoulos *et al.*, "Synchrophasor measurement accuracy characterization," North Amer. SynchroPhasor Initiative Performance & Standards Task Team, , 2007.

[22] C. Na, D. Obradovic, and R. Scheiterer, "A probabilistic approach to clock synchronization of cascaded network elements," in *Proc. ICASSP*, Apr. 2009, pp. 1793–1796.

[23] G. Giorgi and C. Narduzzi, "Performance analysis of Kalman-filter-based clock synchronization in IEEE 1588 networks," *IEEE Trans. Instrum. Meas.*, vol. 60, no. 8, pp. 2902–2909, Aug. 2011.

[24] M. Kezunovic, A. Sprintson, J. Ren, and Y. Guan, "Signal processing, communication, and networking requirements for synchrophasor systems," in *Proc. 13th Int. Workshop on Signal Processing Advances in Wireless Commun.*, Jun. 2012, pp. 464–468.

[25] P. Top, M. Bell, E. Coyle, and O. Wasynczuk, "Observing the power grid: Working toward a more intelligent, efficient, and reliable smart grid with increasing user visibility," *IEEE Signal Process. Mag.*, vol. 29, no. 5, pp. 24–32, Sep. 2012.

[26] L. Glielmo, P. Marino, R. Setola, and F. Vasca, "Parallel Kalman filter algorithm for state estimation in bilinear systems," in *Proc. 33rd Conf. Decision and Control*, Dec. 1994, pp. 1228–1229.

[27] A. Gomez-Exposito, C. Gomez-Quiles, and A. d. l. V. Jaen, "Bilinear power system state estimation," *IEEE Trans. Plasma Sci.*, vol. 27, no. 1, pp. 493–501, Feb. 2012.

[28] C. Gomez-Quiles, H. Gil, A. de la Villa Jaen, and A. Gomez-Exposito, "Equality-constrained bilinear state estimation," *IEEE Trans. Plasma Sci.*, vol. 28, no. 2, pp. 902–910, Apr. 2013.

[29] N. Shivakumar and A. Jain, "A review of power system dynamic state estimation techniques," in *Proc. Joint Int. Conf. Power Syst. Technol./ IEEE Power India Conf.*, Oct. 2008, pp. 1–6.

[30] H. Beides and G. Heydt, "Dynamic state estimation of power system harmonics using Kalman filter methodology," *IEEE Trans. Power Del.*, vol. 6, no. 4, pp. 1663–1670, Oct. 1991.

[31] G. Valverde and V. Terzija, "Unscented Kalman filter for power system dynamic state estimation," *IET Gen., Transm. Distrib.*, vol. 5, no. 1, pp. 29–37, Jan. 2011.

[32] B. D. Moor, "Structured total least squares and L_2 approximation problems," *Linear Algebra Applicat.*, vol. 188-189, no. 0, pp. 163–205, 1993.

[33] G. H. Golub and C. F. v. Loan, "An analysis of the total least squares problem," *SIAM J. Numer. Anal.*, vol. 17, no. 6, pp. 883–893, 1980.

[34] A. Wiesel, Y. Eldar, and A. Yeredor, "Linear regression with Gaussian model uncertainty: Algorithms and bounds," *IEEE Trans. Signal Process.*, vol. 56, no. 6, pp. 2194–2205, Jun. 2008.

[35] B. Recht, M. Fazel, and P. Parrilo, "Guaranteed minimum-rank solutions of linear matrix equations via nuclear norm minimization," *SIAM Rev.*, vol. 52, no. 3, pp. 471–501, 2010.

[36] B. Schaffrin and H. B. Iz, "Towards total Kalman filtering for mobile mapping," in *5th Int. Symp. on Mobile Mapping Technol.*, Padua, Italy, Dec. 2007.

[37] C. E. Davila, "Recursive total least squares algorithms for adaptive filtering," in *Proc. Int. Conf. Acoust., Speech, Signal Process.*, Apr. 1991, pp. 1853–1856.

[38] T. Basar and G. J. Oldser, *Dynamic Noncooperative Game Theory*. London, U.K.: Academic, 1989.

Peng Yang (S'11) received the B.Sc. degree from the University of Science and Technology of China, Hefei, China, in 2009, and the M.Sc. degree from Washington University in St. Louis, St. Louis, MO, USA, in 2011, both in electrical engineering. He is currently working toward the Ph.D. degree in electrical engineering at Washington University in St. Louis under the guidance of Dr. A. Nehorai.

His research interests include statistical signal processing, optimization, machine learning, and compressive sensing, with applications to smart grid.

Zhao Tan (S'12) received the B.Sc. degree in electronic information science and technology from Fudan University of China in 2010. He is currently working towards a Ph.D. degree with the Preston M. Green Department of Electrical and Systems Engineering at Washington University in St. Louis, under the guidance of Dr. Arye Nehorai. His research interests are mainly in the areas of statistical signal processing, radar signal processing, sparse signal reconstruction, optimization theory and smart grid.

Ami Wiesel (M'07) received the B.Sc. and M.Sc. degrees from Tel-Aviv University, Tel Aviv, Israel, in 2000 and 2002, respectively, and the Ph.D. degree from the Technion—Israel Institute of Technology, Haifa, Israel, in 2007, all in electrical engineering.

He was a Postdoctoral Fellow with the Department of Electrical Engineering and Computer Science, University of Michigan, Ann Arbor, MI, USA, from 2007 to 2009. Since Jan. 2010, he has been a Faculty Member with the Rachel and Selim Benin School of Computer Science and Engineering, Hebrew University of Jerusalem, Jerusalem, Israel.

Dr. Wiesel was a recipient of the Young Author Best Paper Award for a 2006 paper in the IEEE Transactions on Signal Processing and a Student Paper Award for a 2005 Workshop on Signal Processing Advances in Wireless Communications (SPAWC) paper. He was awarded the Weinstein Study Prize in 2002, the Intel Award in 2005, the Viterbi Fellowship in 2005 and 2007, and the Marie Curie Fellowship in 2008.

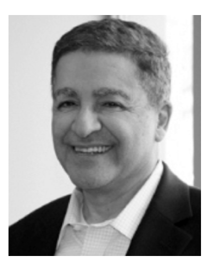

Arye Nehorai (S'80–M'83–SM'90–F'94) received the B.Sc. and M.Sc. degrees from the Technion, Haifa, Israel, and the Ph.D. degree from Stanford University, Stanford, CA, USA.

He is the Eugene and Martha Lohman Professor and Chair of the Preston M. Green Department of Electrical and Systems Engineering, Washington University in St. Louis, St. Louis, MO, USA. Earlier, he was a faculty member with Yale University and the University of Illinois at Chicago.

Dr. Nehorai is a Fellow of the Royal Statistical Society and the AAAS. He served as editor-in-chief of the IEEE TRANSACTIONS ON SIGNAL PROCESSING from 2000 to 2002. From 2003 to 2005 he was the Vice President of the IEEE Signal Processing Society, the Chair of the Publications Board, and a member of the Executive Committee of this Society. He was the founding editor of the special columns on Leadership Reflections in the *IEEE Signal Processing Magazine* from 2003 to 2006.